

Gamma-Ray Astronomy with the CGRO/BATSE Instrument

First Year Report

A. B. Hill

University of Southampton

Abstract

Aspects of gamma ray astronomy with the Burst And Transient Source Experiment are discussed. An overview of the standard analysis techniques and their associated difficulties is performed. The new techniques developed at Southampton, flat-fielding by Mass Modelling and Likelihood imaging, are described and the first results investigated. Additionally the first preliminary spectral data sets are presented. Future work discussed includes investigating the BATSE spectra and pursuing the complete flat-fielding of the BATSE data set. In addition the application of INTEGRAL observation time for targets of interest from the BATSE data is considered.

1. Introduction

The Compton Gamma Ray Observatory (CGRO) was one of NASA's Great Observatories. Successfully launched in April 1991 it operated in low Earth orbit (LEO) for over 9 years until it was de-orbited in June 2000 (Harmon et al. 2002). Four instruments were carried aboard the CGRO: the Energetic Gamma Ray Experiment (EGRET); the Imaging Compton Telescope (COMPTEL); the Oriented Scintillation Spectrometer (OSSE); the Burst and Transient Source Experiment (BATSE). Between them these four instruments spanned an energy range from 30 keV to 30 GeV. The CGRO orbital period was approximately 90 minutes and the orbital inclination was 28° , with a precession period of ~ 53 days.

1.1 BATSE

BATSE consisted of eight uncollimated 2025 cm^2 NaI(Tl) Large Area Detectors (LADs) each located on one corner of the CGRO satellite. They were sensitive to photons within the energy range $20 \text{ keV} - 2 \text{ MeV}$ and had a field of view of 4π steradians (Fishman et al. 1989a). Data was recorded in two formats: the DISCLA data, consisting of 4 energy channels recorded in 1.024 second bins; the CONT data, consisting 16 energy channels recorded in 2.048 second bins. BATSE was designed primarily to detect Gamma Ray Bursts (GRBs).

1.2 Earth Occultation Analysis

Before the launch of the CGRO it was realised that the Earth would act as an occulting disc throughout the orbit allowing BATSE to observe non-transient sources. The BATSE LADs will observe a step-like feature in the measured count rate as a source crosses the Earth's limb. This is due to the gradual attenuation of the gamma ray flux with the increasing column density of the Earth's atmosphere. As a source sets behind the Earth there is a drop in the LAD count rate and as it rises there is an increase.

During the course of an entire precession all sources on the sky will undergo occultation although high-declination sources, $|\delta| \geq 41^\circ$, near the celestial poles receive less coverage than the rest of the sky. Including data losses this means that between 50% and 90% of the sky can be observed in any 53 day period (Shaw et al. 2003).

1.2.1 Step Searching

Knowledge of the time a source is occulted translates into knowledge of the source position on the sky by applying the known orientation and location of the CGRO and the Earth's limb. This allows a location accuracy of $\sim 1^\circ$. Techniques were developed at Marshall Space Flight Centre (MSFC) to exploit this and to search the BATSE data set for step-like occultation features (Harmon et al. 2002). This technique of searching for steps in the count rate is limited by the difficulty in accurately estimating the background

as well as non-statistical noise which is introduced by bright pulsating sources with periods of the order of minutes.

1.2.2 Step Fitting

The fluxes of known sources can also be measured. By measuring the height of the step feature above the background the flux of the source is directly measured. This is achieved by simultaneously fitting a quadratic polynomial to the detector background and a step function to the source being measured as well as to any additional sources which may interfere to the count rate of each energy channel in each LAD independently. The Earth's limb has a diameter of $\sim 140^\circ$ as seen from BATSE and so any other source which lies on the limb with that being measured can contaminate the flux measurement unless it too is fitted. This is achieved by fitting over a window of ~ 230 seconds, with the occultation step occurring in the middle of the window. Theoretically the statistical uncertainty of the measurement can be improved by considering a larger window to fit to; this is impractical as it is limited by the background fit and over longer timescale may introduce additional slower background variations requiring a more complex model. There is also an increased probability of encountering additional steps from unknown sources (Shaw et al. 2003).

1.2.3 Occultation Imaging

Neither of these techniques images the gamma ray sky. The timing of occultation features can be transformed into spatial information which can be applied to the creation of images. This was an improvement over the step searching routine for locating and identifying weaker sources as well as increasing the ability for BATSE to discriminate in crowded regions such as the galactic centre (Harmon et al. 2002). The arcing limb of the Earth is projected onto the sky. As the Earth's limb moves across the sky the LADs record the count rate as a function of time and when a point source crosses the limb a step feature occurs in the count rate. The orientation of the limb changes as the spacecraft precesses in its orbit. Hence over enough orbits the intersection point of the Earth's limb reveals the position of the source. The occultation transform imaging technique applies

the Radon transformation and the maximum entropy methods. This has proved successful in locating new transient sources to within less than 0.5° accuracy and has allowed the observation of low mass x-ray binaries, active galactic nuclei and supernova remnants.

However, this technique has its limitations which make it unable to generate all-sky images. The inverse Radon transformation assumes the Earth's limb to be linear and so limits sky images to be a maximum of $20^\circ \times 20^\circ$ in size. Also, the maximum entropy method is computationally intensive and limits the number of days which can be combined to make an image to 15-20 days.

2 Current Work

At the University of Southampton techniques have been recently developed to improve the sensitivity of the standard occultation analysis techniques developed at MSFC in addition to producing a true all-sky imaging technique which can be applied to the entire 9 year BATSE data set. A technique to model the background and hence flat field gamma ray detectors has been developed at Southampton. A dynamic Monte Carlo model is used to simulate the dominant components of the gamma ray background throughout the orbit of CGRO. Additionally, a technique to image the entire sky over the full 9 year BATSE lifetime by applying a maximum likelihood method has been developed (Shaw et al. 2001).

2.1 New Techniques

2.1.1 The BATSE Mass Model

The BATSE Mass Model (BAMM) is based on The Integral Mass Model (TIMM), which is a GEANT based Monte-Carlo particle code developed at Southampton to simulate the INTEGRAL mission (Lei et al. 1999). The numerical model is constructed taking into account the detector geometries and chemical. BAMM contains information regarding the entire CGRO spacecraft with specific detail attributed to the BATSE detector

modules (Shaw et al. 2002). The model is initially assumed to be in deep space and bombarded with isotropic particle fluxes. Three types of particles are considered: Cosmic Diffuse (CD) background gamma rays; cosmic rays (CR); atmospheric albedo gamma rays (ATM). Each energy deposit is recorded as well as the entire history of the particle which caused the deposit.

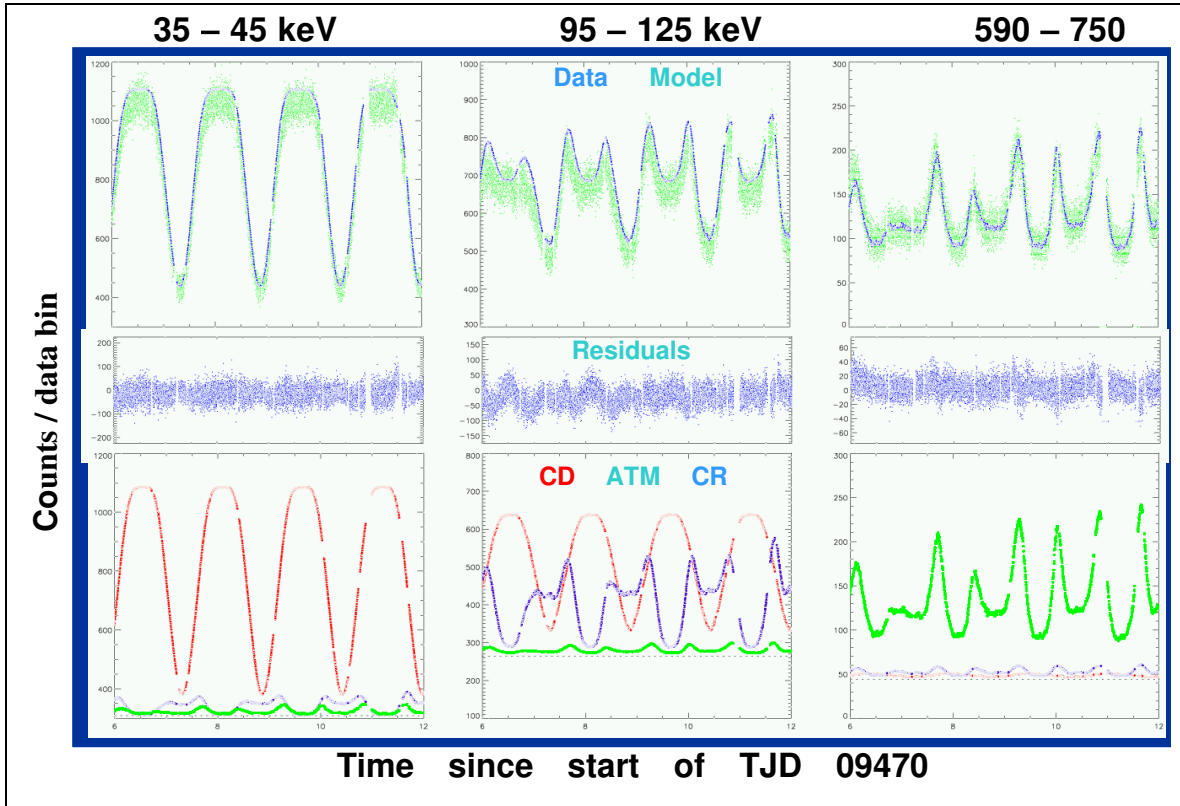


Figure 1: Background components fitted to the data set

BATSE however is in LEO and hence has a highly variable background. The static energy deposit database is now filtered using the criteria of the physical location and orientation of the CGRO. This filtered database is now be used to simulate the background for any orbital position and pointing. This results in the generation of the three components, CD, CR and ATM. These are then summed together to estimate the overall background. However due to uncertainty in the input spectra the results of the mass modelling cannot exactly reproduce the count rates measured in the BATSE detectors (Shaw et al. 2002). The background shape is accurately reproduced but it requires normalization. A section of data for each detector and energy channel, at the

time period of interest, which is free from additional contamination from sources such as the South Atlantic Anomaly, is selected. The bright gamma ray sources above 200 mCrab brightness are subtracted from this selection of data. The model:

$$C(t) = \alpha \times CD(t) + \beta \times CR(t) + \gamma \times ATM(t) \quad (1)$$

is fitted to the data. The data are flat-fielded by simply subtracting $C(t)$. An example of the individual components and the flat fielded data is shown in Figure 1. To date approximately 500 days of the 9 year BATSE data set have been flat-fielded using this approach.

2.1.2 All Sky Imaging

As discussed in §1.2.3, the standard imaging technique is restricted only to small areas of the sky and so a new approach is required in order to image the entire sky and hence exploit the 4π field of view of BATSE. The Likelihood Imaging Method for BATSE Occultation data (LIMBO) code is a collection of software developed at Southampton to generate long duration all sky maps from the BATSE CONT data set (Knödlseeder 1999; Shaw et al. 2001; Shaw et al. 2003). An image is constructed by using a Maximum Likelihood Ratio (MLR) test for source emission over a pre-defined grid of sky positions. This technique differs from the standard technique in that it produces the results of a number of statistical tests and not a deconvolution of the data.

When considering long sections of BATSE data a good understanding of the gamma ray background is required, hence BMM flat-fielded data is used. The first step in the LIMBO process is to transform the data through a differential filter from a count rate containing occultation steps to a set of occultation peaks. The choice of differential filter is a balance between optimising angular resolution and sensitivity (Shaw et al. 2001). A MLR test is then applied to determine the significance of flux detection at every single point over a grid of positions from the filtered data. The MLR, λ is calculated as the difference:

$$\lambda = C_o - C_{SRC} \quad (2)$$

where C_O and C_{SRC} are the χ^2 statistics for the null and source hypotheses respectively. C_{SRC} contains a response vector which describes the expected shape, position and amplitude as a function of source position and strength and a scaling factor, α which is proportional to the flux received. The likelihood image $\lambda(x,y)$, is constructed by the superposition of the arcs caused by the occultation of sources by the Earth's limbs.

Harmon et al. (2002) investigated the response of each energy channel in each of the eight LADs with varying photon incident angle and energy. The standard technique was used to observe the Crab Nebula over the majority of the CGRO lifetime, during which time the Crab was seen by each of the detectors at a multitude of angles. This allowed the data set to be calibrated to give maps of α in units of the normalised Crab Nebula response.

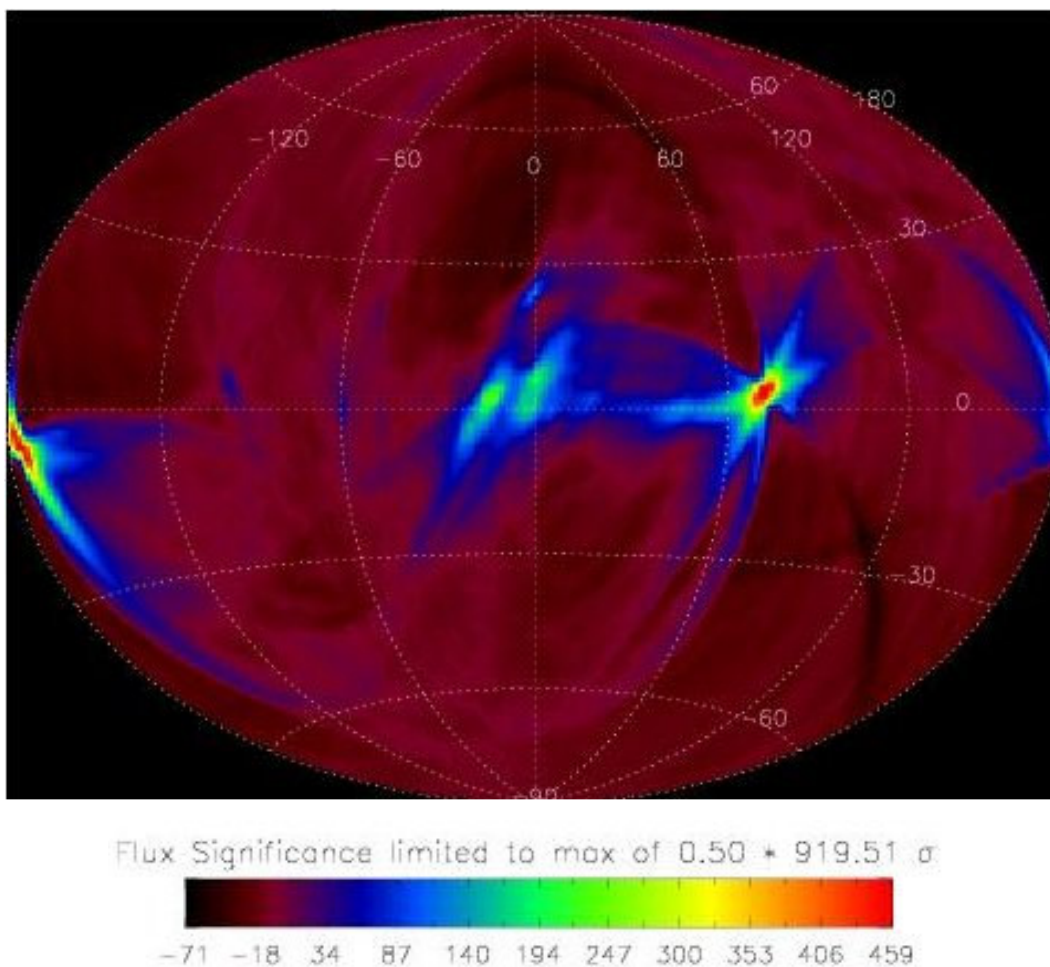


Figure 2: Map of the significance of 25 - 160 keV flux from the whole sky for a total of 489 days from TJD 09448 to 09936 made using LIMBO.

Likelihood maps can be made for short periods of time and then can be added together to increase source significance. An all-sky map for 489 days in the period TJD 09448 – 09936, produced from 7 CONT energy channels (25 – 160 keV) has now been compiled and is shown in Figure 2. It has a 3σ statistical sensitivity of 3 mCrab and can be considered the first all-sky gamma ray image to be generated since the HEAO1-A4 mission. This map attempts to maximise the significance of detection of sources. In addition to this map seven individual maps for the same time frame, but separated into each of the 7 energy channels, have been generated. However it can be seen that the brightest sources on the sky, such as the Crab Nebula and Cygnus X-1, produce bright artefacts on these maps. These artefacts are images of the Earth's limb. Source location improves as more limbs are superimposed and the likelihood peak increases, however the remnants of the limbs for bright sources may be more significant than the likelihood peak of a weaker source which lies on the path of the limb. As the limb of the Earth is $\sim 140^\circ$ this is a very large effect. In addition to this artefacts in crowded regions, such as the Galactic Centre, results in source confusion.

2.1.3 Image Artefact Removal

As seen in §2.1.2 the artefacts in LIMBO images are certainly significant and need to be removed to maximise the usefulness of the LIMBO imaging process. An approach similar to the CLEAN algorithm applied to radio interferometry has been developed. From the knowledge of the CGRO orbit and the detector pointing the time, shape and size of a BATSE occultation limb can be calculated. As the artefacts in the LIMBO images are a result of the superposition of occultation limbs caused by point sources it is possible for a Point Spread Function (PSF) for any position of the sky to be generated based on the history of the Earth's limb (Shaw et al. 2003). This PSF can then, in theory be removed from the LIMBO map and the integral flux deposited into a clean map in the same position but with a more ideal PSF such as a Gaussian. The cleaning algorithm searches the map for the brightest pixel and cleans a fraction of the flux at this point before moving onto the next brightest pixel until a pre-defined limit is reached. Once

completed the residual LIMBO map should contain nothing but background noise and should be added back to the cleaned components to produce the final map.

A requirement of the CLEAN algorithm is that the imaging property being reduced is linear. The MLR, however, is not linear but is based on a geometrical sum. The numerator of the scaling factor α is linear and the denominator is constant and so it is possible to run the cleaning algorithm on the numerator and use the results of this to derive the cleaned flux and likelihood maps. If the PSF is subtracted from the wrong place then systematics will be added into the map. As the LIMBO map is constructed of pixels $2^\circ \times 2^\circ$ the brightest pixel does not necessarily correspond to the correct source position and hence the wrong PSF will be subtracted. To combat this known bright sources are pre-cleaned using their known positions and subtracting a large fraction (~95%) of their flux before iterating around the map (Westmore 2002).

To date, the maps described at the end of §2.1.2 have all been cleaned using this process typically down to at least 3σ , although the higher energy maps have not been cleaned down quite this far due to poorer performance at the higher energies. Through this process the PSFs for all of the statistically significant sources have been generated for the 489 day period which matches the maps and for each energy channel in the range 2-8. The PSF is variable with energy and appears to change relatively insignificantly at the lower energy channels but more significant at the higher energy channels. As a result individual energy maps had their own PSFs generated. In the case of maps summed over energy channel we have had to assume that the lower energy PSF will be dominant and apply this to the map.

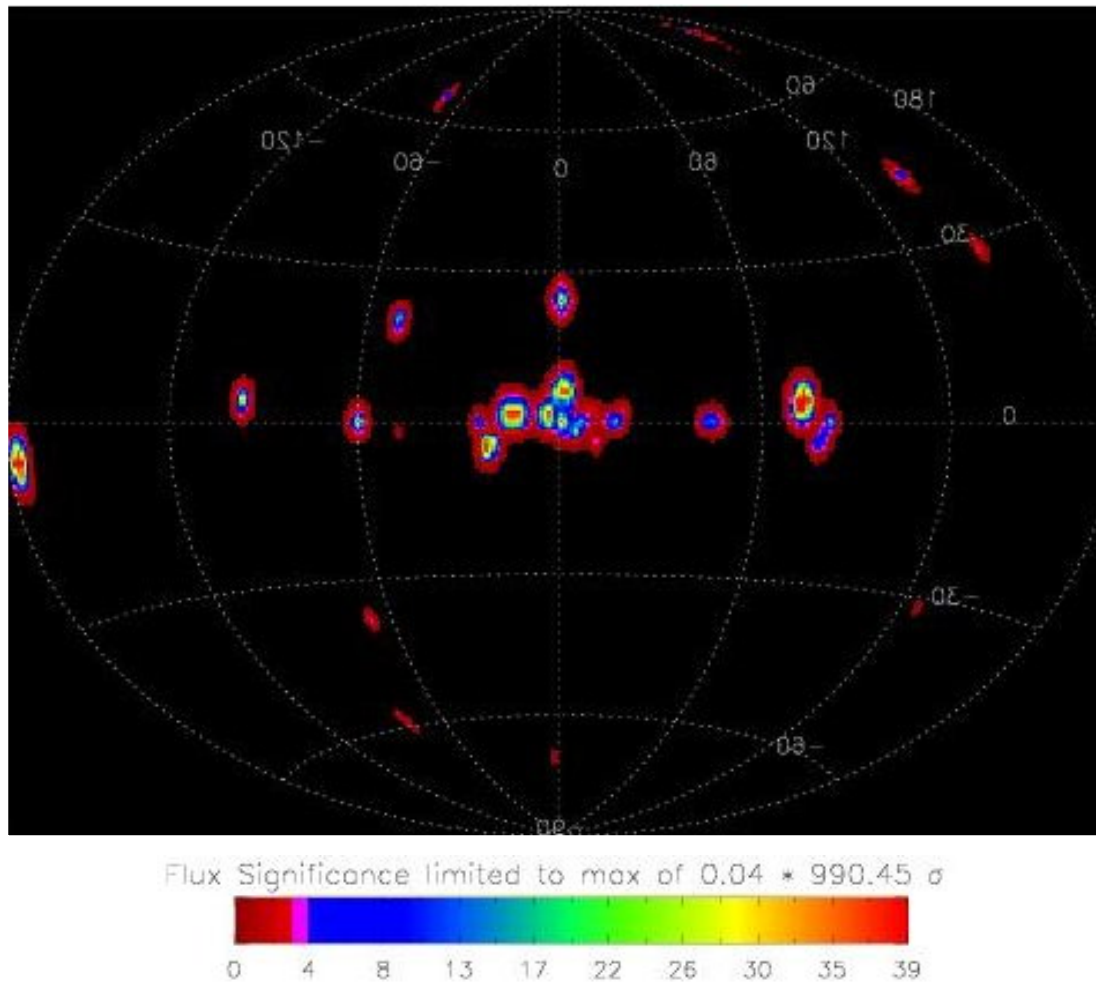


Figure 3: The results of performing the image cleaning technique on the all-sky map of Fig. 2. (Cleaned components only). See tables 1 and 2 for a summary of the identified sources from the image.

2.2 Results

2.2.1 All Sky Source Catalogue

The cleaned 489 day, 7 CONT energy channel map shows the detection significance of the Crab Nebula to be 990σ . This gives a 5σ sensitivity of ~ 5 mCrab. In order to extract sources from the map the SExtractor 2.2.2 (SE) software, developed by Bertin & Arnouts (1996) was used. A detection threshold of 1σ , cleaning efficiency of 1.0 and a wavelet pass-band filter were applied in order to guarantee that all sources were extracted whilst

obvious false detections could be discarded. An ISO_CORR aperture was used for photometry.

Two maps were generated to use with SE; one contained only the cleaned components and one contained the cleaned components added back to the residual flux. The latter is the more scientifically accurate map and running the SE software on it rendered the catalogue of detections shown in Table 1. The fluxes of the sources listed have been normalised to the Crab flux. The source detections were compared against a list of sources compiled from the HEAO1-A4 (Levine et al. 1984) catalogue, BATSE persistent and transient sources (Harmon et al. 2001; Ling et al. 2000) as well as a catalogue of gamma ray selected AGN (Malaguti 1999). Any source which lies within 2.8° of its known position is within the diagonal size of one image pixel. If no known source has been detected within a radius of 5.7° the detection has been marked as ‘unknown’.

Table 1: List of sources detected in the 25 - 160 keV band for the period TJD 09448 - 09936.

Measured Position (l,b)	Source Name	Known Position (l,b)	Position Error (degs)	Flux (mCrab)
(71.9, 3.8)	Cygnus X-1	(71.34, 3.07)	0.9	1142 ± 18
(-175.9, -5.9)	Crab	(-175.44, -5.78)	0.5	1000 ± 17
(0.0, 6.9)	GRO J1749-24	(0.18, 7.02)	0.2	214 ± 9
(-12.0, 2.0)	4U 1700-377	(-12.2, 2.2)	0.3	209 ± 8
	GX 349+2	(-10.90, 2.74)	1.3	
(-2.0, 0.9)	1E 1740-29	(-0.9, -0.1)	1.5	201 ± 9
	GX 359+2	(-0.43, 1.56)	1.6	
(0.0, 0.2)	GRO J1740-29	(0.0, 0.3)	0.1	180 ± 8
	XTE J1748-288	(0.7, -0.2)	0.8	
	1E 1740-29	(-0.9, -0.1)	1.0	
	GRS 1739-278	(0.67, 1.18)	1.2	
	GX 359+2	(-0.43, 1.56)	1.4	
(-16.0, 2.0)	GRO J1655-40	(-15.02, 2.46)	1.1	128 ± 7
	OA0 1657-415	(-15.8, 0.4)	1.6	
(0.1, 24.0)	Sco X-1	(0.90, 23.78)	1.0	114 ± 7
(-21.5, -4.7)	GX 339-4	(-21.05, -4.32)	0.6	93 ± 6

(-96.3, 3.7)	Vela X-1	(-96.94, 3.93)	0.7	83 ± 6
(16.7, 1.4)	GX 17+2	(16.44, 1.28)	0.3	77 ± 8
(122.0, -30.0)	Unknown	(-, -)	-	51 ± 8
(4.6, -1.4)	GX 5-1	(5.07, -1.02)	0.6	46 ± 5
(44.34, 0.0)	1907+097	(43.6, 0.2)	0.7	43 ± 5
	GRS 1915+105	(45.40, -0.23)	1.1	
(-2.0, 6.0)	GRO J1719-24	(0.18, 7.02)	2.4	42 ± 5
(-60.0, 0.0)	GX 301-2	(-59.90, -0.03)	0.1	42 ± 4
(80.0, 0.6)	Cygnus X-3	(79.84, 0.71)	0.2	36 ± 5
(-50.00, 19.5)	Centaurus A	(-50.39, 19.46)	0.5	33 ± 5
(-158.83, -4.0)	4U 0614+091	(-159.11, -3.38)	0.7	31 ± 8
(-24.00, 0.0)	1624-490	(-25.1, -0.3)	1.0	17 ± 3
	4U 1630-47	(-23.09, 0.26)	1.1	
(156.00, 76.0)	NGC 4151	(155.08, 75.06)	1.0	16 ± 3
(138.0, 42.0)	M 82	(141.41, 40.57)	2.9	14 ± 3
(-70.00, 66.0)	3C273	(-70.05, 64.36)	1.8	12 ± 3
(-2.0, -70.0)	Unknown	(-, -)	-	9 ± 3

A number of sources which are visible in the cleaned map were not, however, detected by SE. The cleaned components only map, comprising of the positions where PSFs were removed, was used to guide SE in its source extraction of the cleaned + residuals map. This method assumes that the cleaned detections are real. Fake sources added at random positions in the ‘guiding’ map yielded results which had essentially zero flux and could be discarded as erroneous. Hence guiding the source extraction should not produce false detections. The measured fluxes of these sources are shown in Table 2. As they cannot be independently measured they may not be entirely reliable but indicate the possibility of a detection. It does result in the detection of EXO 2030+375 in addition to Cyg X-1 and Cyg X-3; also indicated is that the distribution of the flux in this region is such that Cyg X-3 and EXO 2030+375 are of comparable brightness.

Table 2: Additionally detected sources.

Measured Position (l,b)	Source Name	Known Position (l,b)	Position Error (degs)	Flux (mCrab)
(-79.0, -59.0)	ESO198-G24	(-88.4, -57.9)	5.0	62 ± 8
(-5.0, -70.0)	NGC 7582	(-11.92, -65.70)	5.0	55 ± 8
(146.1, 28.0)	MKN 78	(151.1, 29.78)	4.7	40 ± 6
(-68.0, -38.0)	Unknown	(-, -)	-	38 ± 6
(-47.9, -2.0)	2S1417-624	(-46.98, -1.60)	1.0	28 ± 5
(76.8, -2.0)	EXO 2030+375	(77.15, -1.24)	0.8	22 ± 5

A number of the primary detections can be seen to have multiple possible associations with sources. These are typically in the crowded Galactic Centre region and it is a result of the coarse $2^\circ \times 2^\circ$ pixel size. The possibility exists to refine this to a $0.5^\circ \times 0.5^\circ$ pixel sized map, however although potentially increasing angular resolution it would be extremely computationally intensive.

2.2.2 Spectra

By splitting the 489 day map into its component energy channels the possibility of extracting spectral information for any position on the sky. Each of the 7 CONT energy channels combined in the summed map were cleaned down as far as feasible. The majority of the channels were cleaned down to 3σ or less; 10 mCrab corresponds to a detection of above 3σ in each of the energy channels. The channel widths are described in Table 3. The source catalogue from §2.2.1 was used to guide SE to extract out the sources in each of the 7 individual energy maps. This guarantees that source information is extracted from the exact same position in every energy channel and that a complete sample is taken across the energy range.

A piece of IDL code combines the photometry from each of the individual energy maps and compiles it into spectral information for each individual source. As all of the flux information is in the form of Crabs this data must be converted to more useful spectral

units. This is achieved by dividing data by the Crab spectrum which was used by Harmon et al. (2002) to normalise the response function as discussed in §2.1.2. This used the Crab spectrum measured by HEAO1-A4 (Jung 1989). The preliminary rough plots of these data sets can be seen in Appendix A.

Table 3: Energy equivalent to CONT channel number.

CONT Energy Channel	Energy (keV)
2	30 – 40
3	40 – 50
4	50 – 70
5	70 – 100
6	100 – 120
7	120 – 160
8	160 – 230

Upon inspection the preliminary plots look promising. Expected soft (hard) sources show soft (hard) spectra and the error bars generally remain small until the detection approaches the 3σ limit. In order to perform any rigorous analysis on the spectra more developmental work needs to be done, however some preliminary analysis may be performed on a number of sources.

2.2.2.1 GX 339-4

On inspection it can be seen that GX339-4 stands out as a consistently bright source across all of the energy bands sampled. It is a black hole candidate which spends most of its time in the low/hard state. If we assume that the spectrum behaves as a simple power law then a straight forward linear fit yields a photon index of 1.88 with a reduced χ^2 of ~ 2.09 . This falls within the range of ~ 1.5 - 2.0 described in Kong et al. (2001) for the low/hard state. The spectrum and fit are shown in Figure 4.

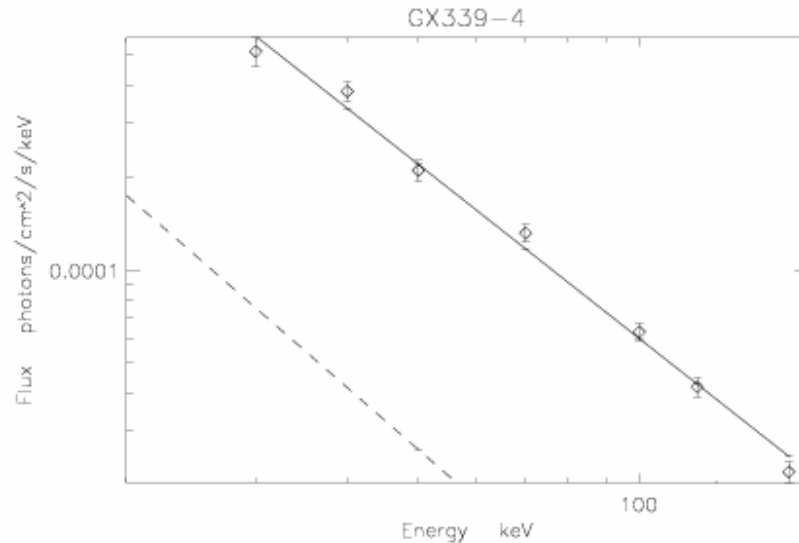


Figure 4: The preliminary spectrum of GX 339-4. The solid line represents a best fit power law with index -1.88. The dashed line represents a 3 sigma detection limit.

2.2.2.2 Centaurus A

Cen A is the nearest AGN to us and is classified as a Seyfert 2 object. Qualitatively it can be seen that Cen A exhibits a hump in its spectrum between 40 and 70 keV, see Appendix A. A similar feature is observed by Benlloch et al. (2001) when observing Cen A over three different epochs with RXTE. It is interesting to note that their errors in that energy range are large relative to ours which leaves the possibility that with further analysis we may be able to refine the parameters of their model.

2.2.2.3 M 82

M82 is a prototypical starburst galaxy, with expected gamma ray emission due to the high supernova rate. M82 appeared as a detection in the 489 day, 25 – 160 keV map catalogue in §2.2.1. It is an interesting detection as BATSE has previously not observed it. The spectrum it produces is also intriguing as it appears to have no emission above the 3σ limit at energies lower than 70 keV. The M82 detection however does fall outside of a single pixel diameter and so could be a different source.

3 Further Work

The work discussed here will continue in several different areas. Maximising the science which can be extracted from the current data set is common to most of the future work although new areas shall be explored.

3.1 BATSE Background Generation

Currently the three individual components which make up the background model for BATSE have been generated for the entire 9 year data set. However the measurements of the flux of bright sources (>200 mCrab) are currently only available for the ~ 500 day period which has been fitted and for which the LIMBO and cleaning codes have been run. Now that the software has been fully proven it is hoped that the flux measurements for the rest of the data set will be supplied by MSFC. With this data in hand it will be possible to fit the BAMB to all of the data and have a flat-fielded 9 year data set. This can then be used for the generation of more sensitive, longer duration LIMBO maps and also be used with the standard occultation technique to increase sensitivity.

3.2 The Standard Occultation Technique

The standard technique can now be used to construct a 9 year light curve of the additional sources which have been found through the LIMBO cleaned map. This will allow us to confirm the sources as real as well as produce useable scientific data. Specific targets to investigate are M82, NGC 6251, Cyg A as well as investigating EGRET sources just above the Galactic Centre in the vicinity of the anti-matter fountain. These measurements will form the base of observation proposals for the INTEGRAL AO-2.

3.3 LIMBO Imaging

Once the entire data set has been flat-fielded it will be possible to compile longer duration maps. In addition a refined $0.5^\circ \times 0.5^\circ$ pixel sized map will be generated in one of the lower energy bands and cleaned. The objective here is to maximise the number of

potential detections whilst refining our angular resolution whilst minimising the amount of CPU time required. Confirmed new sources with their improved locations may be submitted for INTEGRAL observations.

3.4 BATSE Spectra

In order to fully analyse the BATSE spectra they need to be read into an appropriate spectral fitting package such as, XSPEC. However, XSPEC expects a detector response matrix to be applied to the data set. As the LIMBO code has already normalised all of the detector responses a null Response Matrix File (RMF) needs to be generated before complex spectral models can be fitted to the current data sets.

The intention is to investigate the brightest sources which have been sampled by other instruments and hence confirm that the spectral measurements are accurate before investigating the weaker sources. The possibility exists to explore spectral variability of the brighter sources. Additionally there is the possibility that sources are detected in individual energy channels which have are not detected in the summed 489 day, 25 – 160 keV map. These need to be extracted individually using the SE code.

Using the standard BATSE spectral software we intend to compile composite Seyfert I and Seyfert II spectra.

4 References

- Bhattacharya, D., The, L.-S., Kurfess, J. D., et al. 1994, *ApJ*, 437, 173
- Benlloch, S., Rothschild, R. E., Wilms, J. et al. 2001, *A&A*, 371, 858
- Bertin, E. & Arnouts, S. 1996, *A&AS*, 117, 393
- Fishman, G. J., Meegan, C. A., Wilson, R. B., et al. 1989a, in *Gamma Ray Observatory Science Workshop*, Goddard, Greenbelt, ed. N. Johnson, Vol. 2, 39-50
- Harmon, B. A., Fishman, G. J., Wilson, C. A., et al. 2002, *ApJS*, 138, 149
- Harmon, B. A., Wilson, C. A., Fishman, G. J., et al. 2001, *American Astronomical Society Meeting*, 199, 0
- Jung, G. V. 1989, *ApJ*, 338, 972
- Kong, A. K. H., Charles, P. A., Kuulkers, E., et al.. 2002, *MNRAS*, 329, 588
- Knödseder, J. 1999, *BATSE All-sky Imaging using Earth Occultation*, Tech. Rep. BATSE-RP-CESR-1: 2, Centre d'Etude Spatiale des Rayonnements, Toulouse
- Lei, F., et al. 1999, *Astrophys. Lett. Commun.*, 39, 373
- Levine, A. M., Lang, F. L., Lewin, W. H. G., et al. 1984, *ApJS*, 54, 581
- Ling, J. C., Wheaton, W. A., Wallyn, P., et al. 2000, *ApJS*, 127, 79
- Malaguti, G. 1999, *Catalogue of extragalactic sources for the IBIS instrument*, Tech. Rep. IN-IM-TES-RP-0027, Insitituto TESRE/CNR, Bolgna
- Shaw, S. E., Bird, A. J., Dean, A. J. et al. 2001, in *Exploring the Gamma-Ray Universe: Proceedings of the 4th INTEGRAL Workshop*, Alicante, 2000, ed. A. Gimenez, V. Reglero, & C. Winkler, Vol. ESA SP-459, 521-524
- Shaw, S. E., Westmore, M. J., Bird, A. J., et al. 2002, *A&A*, 398, 391
- Shaw, S. E., Westmore, M. J., Hill, A. B., et al. 2003, in preparation
- Westmore, M. J. 2002, *PhD thesis*, Dept. of Physics and Astronomy, University of Southampton, UK., Submitted October 2002
- Wilms, J., Nowak, M. A., Dove, J. B., et al. 1999, *ApJ*, 522, 460

5 Appendix A

The following pages display the preliminary spectral data obtained from the cleaned 489 day (TJD 09448 – 09936) LIMBO maps of the CONT energy channels 2 – 8 covering the range 30 – 160 keV. Due to the simplicity of the plots the data point for each energy channel is aligned with the start energy of that channel as listed in Table 3. If an ID for each source has been possible the name of the source has been placed in the title, any unknown sources are listed as such. The order of the plots is identical to the order of sources listed in the catalogue shown in Table 1. For information on the position of extraction and source confusion in the region the catalogue should be referenced.

The data points are displayed with their associated error bars. The dashed line represents a 10 mCrab limit. This limit is above the 3σ detection limit in each of the energy channels and so any detection above this line is a believable detection. Any data point on or below the line, then the line should be taken as an upper detection limit.